then the average value of A_4 is 0.36 in the case of all the results and 0.34 if only the more reliable[15] results on the swollen networks are included. On the other hand, if for example the reaction were only 50% complete (partly because of Pd-oxidized removal of acac groups), then M_c would be effectively doubled and A_4 would be 0.72 or 0.68. These values are in satisfactory agreement with the theoretical value 0.50 predicted for tetrafunctional networks;[5,15-17] none of the values provides evidence for significant contributions from interchain entanglements, which is in agreement with results obtained on a variety of other elastomeric systems.[5,15,18] The values obtained for the ratio $2C_2/2C_1$ average to 0.86 for the unswollen networks and 0.44 for the swollen ones and are of the same magnitude as values reported for a variety of other tetrafunctional networks.[13]

Values of the elongation at rupture (maximum extensibility) and ultimate strength (as represented by the reduced stress at rupture) are given in columns seven and eight of Table I. These values of the ultimate properties indicate that the chelation networks are quite good elastomers. Increases in reduced stress above the linear continuations of the curves are given in the final column of Table I. As can be seen from these tabulated results and from Figures 1 and 2, the reinforcing upturns in $[f^*]$ are little affected by increase in temperature or increase in degree of swelling. This indicates that they are due to the limited extensibility of the network chains[5,19] rather than to strain-induced crystallization.[20] The achievement of sufficiently high elongations to observe such an effect attests to the relatively high degree of perfection in these network structures. The present results thus encourage additional investigations of other elastomeric properties of these and other chelation networks.

Acknowledgment. It is a pleasure to acknowledge the financial support provided J.E.M. by the National Science Foundation through Grant DMR 79-18903-03 (Polymers Program, Division of Materials Research) and B.E.E. by the Department of Energy through Contract DE AT06-81 ER10912.

Registry No. Palladium acetate, 3375-31-3.

References and Notes

(1) Flory, P. J. "Principles of Polymer Chemistry"; Cornell University Press: Ithaca, NY, 1953.
(2) Treloar, L. R. G. "The Physics of Rubber Elasticity"; Clarendon Press: Oxford, 1975.
(3) Mark, J. E. *J. Chem. Educ.* **1981**, *58*, 898.
(4) "Elastomers and Rubber Elasticity"; Mark, J. E., Lal, J., Eds.; American Chemical Society: Washington, DC, 1982.
(5) Mark, J. E. *Adv. Polym. Sci.* **1982**, *44*, 1.
(6) Yeh, H. C.; Eichinger, B. E.; Andersen, N. H. *J. Polym. Sci., Polym. Chem. Ed.* **1982**, *20*, 2575.
(7) Iwamoto, N.; Eichinger, B. E.; Andersen, N. H., submitted to *Rubber Chem. Technol.*; Iwamoto, N. Ph.D. Thesis, University of Washington, 1983.
(8) Martell, A. E.; Smith, R. M. "Critical Stability Constants"; Plenum Press: New York, 1977; Vol. 3.
(9) Llorente, M. A.; Andrady, A. L.; Mark, J. E. *J. Polym. Sci., Polym. Phys. Ed.* **1981**, *19*, 621.
(10) Mark, J. E.; Sullivan, J. L. *J. Chem. Phys.* **1977**, *66*, 1006.
(11) Llorente, M. A.; Andrady, A. L.; Mark, J. E. *J. Polym. Sci., Polym. Phys. Ed.* **1980**, *18*, 2263.
(12) Mark, J. E.; Flory, P. J. *J. Appl. Phys.* **1966**, *37*, 4635.
(13) Mark, J. E. *Rubber Chem. Technol.* **1975**, *48*, 495.
(14) Llorente, M. A.; Mark, J. E. *J. Chem. Phys.* **1979**, *71*, 682.
(15) Erman, B.; Wagner, W.; Flory, P. J. *Macromolecules* **1980**, *13*, 1554.
(16) Flory, P. J. *Proc. R. Soc. London, Ser. A* **1976**, *351*, 351.
(17) Flory, P. J.; Erman, B. *Macromolecules* **1982**, *15*, 800 and pertinent references cited therein.
(18) Mark, J. E. *Rubber Chem. Technol.* **1981**, *54*, 809.
(19) Mark, J. E.; Curro, J. G. *J. Chem. Phys.* **1983**, *79*, 5705.
(20) Mark, J. E. *Polym. Eng. Sci.* **1979**, *19*, 409.

Development of Modulated Structure during Solution Casting of Polymer Blends†

Takashi Inoue,* Toshiaki Ougizawa, Osamu Yasuda,‡ and Keizo Miyasaka

Department of Textile and Polymeric Materials, Tokyo Institute of Technology, Ookayama, Meguro-ku, Tokyo 152, Japan. *Received February 7, 1984*

ABSTRACT: We have found the development of regularly phase-separated structure in solution-cast films of polymer blends. Characteristic features of the structure are periodicity and dual connectivity of phases. Here we call it "modulated structure". The casting process from ternary solution, consisting of A polymer, B polymer, and solvent, to dry film was studied by using the light scattering technique. The regular structure that developed at relatively low polymer concentration was maintained as a whole at higher concentrations until the modulated structure was frozen in the cast film. More than ten pairs of dissimilar polymers formed the modulated structure. These pairs had fairly small differences in solubility parameters between the component polymers. Faster rates of solvent evaporation yielded a smaller periodic distance in the modulated structure. The rate of phase separation became lower and the periodic distance of the modulated structure became shorter as the blend ratio deviated from 50/50. When the molecular weight of polymer was very high, the system failed to phase-separate during the fast casting, resulting in a homogeneous blend without appreciable composition fluctuations. These results on development of modulated structure were interpreted through thermodynamic and kinetic discussion in terms of molecular and processing variables such as polymer–polymer interaction parameters, blend ratio, degree of polymerization, and rate of solvent evaporation.

Introduction

The solution casting of an incompatible polymer blend generally results in the two-phase morphology having irregular shape and size of domains. Quite recently, we studied the morphology of poly(vinyl chloride)/poly(acrylonitrile-*co*-butadiene) (NBR) blends cast from tetrahydrofuran (THF) solutions. A regularly phase-separated structure with a periodic distance of 1.4 μm was found in a 50/50 blend of PVC and NBR having 26 wt % acrylonitrile.[1,2] Characteristic features of the structure were the periodicity and the dual connectivity of the phases. They are similar in appearance to the phase

† Presented partly at the 31st Polymer Symposium, Society of Polymer Science, Japan, Oct 1982 (*Polym. Prepr., Jpn.* **1982**, *31* (10), 2549) and partly at the 32nd Polymer Symposium, Society of Polymer Science, Japan, Oct 1983 (*Polym. Prepr., Jpn.* **1983**, *32* (7), 1703).

‡ Present address: Toray Co. Ltd., Mishima, Shizuoka 411, Japan.

0024-9297/85/2218-0057$01.50/0

Table I
Polymer Specimens

code	polymer	$\bar{M} \times 10^{-4}$ [a]		SP,[b] $(cal/cm^3)^{1/2}$
		$\bar{M}_w \times 10^{-4}$	$\bar{M}_n \times 10^{-4}$	
PVC	poly(vinyl chloride)	15.5	7.6	9.55[c]
AS-25	poly(acrylonitrile-*co*-styrene) (25/75)	19.4	6.8	9.97[d]
EVA-58	poly(ethylene-*co*-vinyl acetate) (42/58)	10.2	4.6	8.59[d]
IR	polyisoprene	38.8	18.0	8.15[c]
BR	polybutadiene	49.5	5.3	8.38[c]
CR	polychloroprene	38.8	18.0	8.60[c]
SBR-23	poly(styrene-*co*-butadiene) (23/77)	51.0	16.0	8.50[d]
SBR-45	poly(styrene-*co*-butadiene) (45/55)	47.8	15.6	8.70[d]
NBR-26	poly(acrylonitrile-*co*-butadiene) (26/74)	34.4	11.9	9.11[d]
NBR-32	poly(acrylonitrile-*co*-butadiene) (32/68)	34.0	11.8	9.30[d]
NBR-40	poly(acrylonitrile-*co*-butadiene) (40/60)	29.7	9.3	9.73[d]
PMMA	poly(methyl methacrylate)	11.0	5.0	9.50[c]
PS	polystyrene	22.4	8.8	9.12[c]

[a] GPC. [b] Solubility parameters. [c] "Polymer Handbook". [d] Small's method.

structure formed by spinodal decomposition, as demonstrated in thermally induced phase transitions in polymer–polymer systems such as poly(methyl methacrylate)/poly(acrylonitrile-*co*-styrene)[3] and poly(vinyl methyl ether)/polystyrene[4] having the lower critical solution temperature (LCST) and poly(methylphenylsiloxane)/polystyrene having the upper critical solution temperature (UCST).[5] Here we call the structure "modulated structure" as has been done in the fields of inorganic glasses and metals.[6,7] The term originated from the mechanism of spinodal decomposition; i.e., structure is formed by the superposition of the sine waves of composition fluctuation. We preferably use here the term partly for convenience to describe the morphological features of the periodicity and the dual-phase connectivity.

We are not the first to find the modulated structure in solution-cast films of a polymer blend. To our knowledge, the first is Gardner.[8] One can see the modulated structure in his micrograph (Figure 8 in ref 8) of a blend film of butyl rubber/EPDM (ethylene–propylene–diene terpolymer) cast from toluene solution. He described it as a network type of phase separation. However, he did not pay further attention to the structure.

Our fundamental questions on the modulated structure found in the solution-cast films of polymer blends are (1) why and how does the modulated structure develop and (2) what are the molecular and thermodynamic factors affecting the modulated structures? In order to answer the questions, we have studied the casting process from the ternary solution (A polymer/B polymer/solvent) to dry film by using the light scattering technique. We have also investigated the effects of various factors on the process, such as casting speed (rate of solvent evaporation), polymer–polymer compatibility, blend ratio of polymers, and molecular weights of polymers. The results have confirmed our assumption that the modulated structure originates from the spinodal decomposition of the ternary polymer solution at fairly low polymer concentration during the casting. The experimental results will be interpreted in terms of the thermodynamics of the ternary polymer solution and the kinetics of phase separation.

Experimental Procedures

Polymer specimens are commercial ones. Their characteristics are shown in Table I.

A pair of dissimilar polymers were dissolved at 8 wt % of total polymer in the solvent which was commonly good for both polymers. The solution was poured into a shallow glass dish (7 mm deep and 50 mm in diameter) with a flat glass cover. Both the cover and bottom are made of optically flat glass. The depth of solution in the dish was ca. 2 mm. The rate of evaporation was controlled by adjusting the gap between the cover and dish.

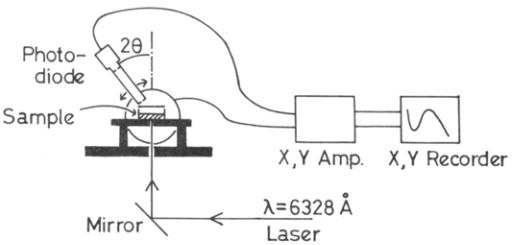

Figure 1. Light scattering apparatus for studying casting of A polymer/B polymer/solvent systems.

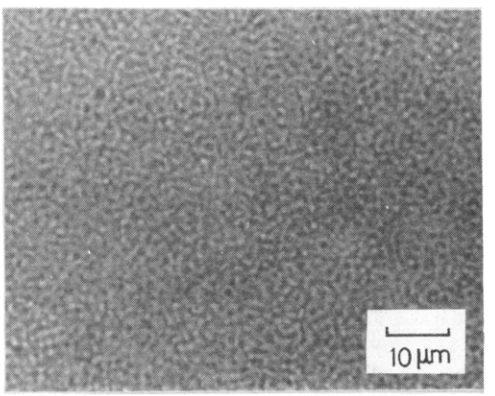

Figure 2. Light micrograph of PVC/NBR-26 blend film obtained by casting process A (see Figure 4a).

The polymer concentration during the casting process was monitored by measuring the weight of the whole dish.

The dish was set horizontally on the light scattering stage as in Figure 1. The radiation of a He–Ne laser of 632.8-nm wavelength was applied vertically to the bottom of the dish. A goniometer trace of the intensity of the scattered light from the solution was given by the light scattering apparatus shown in Figure 1. Thus, the change of light scattering profile was observed during the evaporation (casting) process at 24 °C.

After the polymer concentration had passed 90 wt % and the rate of evaporation had slowed, the concentrated solution was further dried under a vacuum of ca. 10^{-4} mmHg for 10 h. The structure of the dried film was observed under a light microscope. A light scattering pattern (V_v) of the dried film was also obtained by using a photographic technique similar to that of Stein and Rhodes.[9]

Results

Effect of Casting Speed. Figure 2 is a light micrograph of PVC/NBR-26 (50/50) blend film cast from THF solution. The film was cast through a very slow evaporation (process A in Figure 4b). A highly interconnected two-phase morphology with uniform domain size is seen in the micrograph. This characteristic morphological feature is

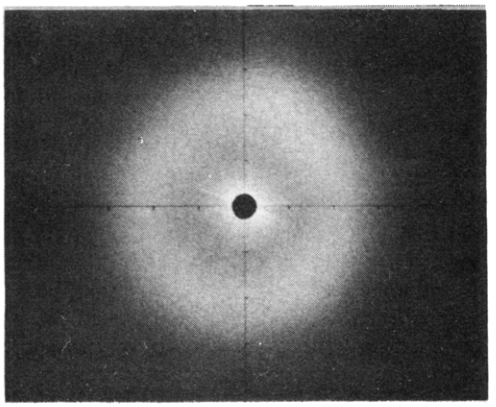

Figure 3. Light scattering pattern (V_v) from PVC/NBR-26 blend film obtained by casting process A (see Figure 4a).

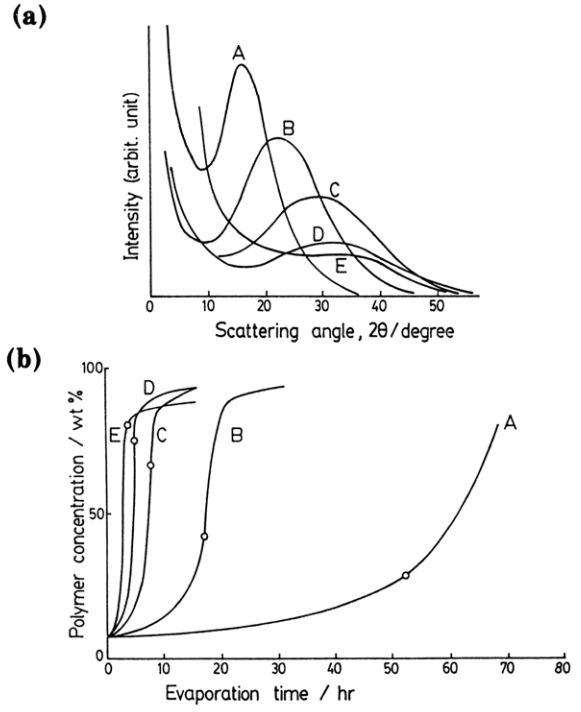

Figure 4. (a) Light scattering profiles from PVC/NBR-26 films obtained at various rates of solvent evaporation. (b) Loss of solvent from films (curves labeled to correspond to those in (a)).

similar in appearance to the structure formed by spinodal decomposition, as demonstrated in thermally induced phase transitions in polymer–polymer systems.[3-5]

Figure 3 shows a light scattering pattern from the cast film of Figure 2. The ring pattern indicates no preferred orientation of the structure in the plane parallel to the film surface. The ring pattern in Figure 3 corresponds to a goniometer trace of the scattered intensity of profile B in Figure 4a. The light scattering peak indicates some degree of regularity of the phase-separated structure in Figure 2. The Bragg spacing from the peak at 16° 2θ is 1.49 μm.

Figure 4a shows light scattering profiles from the cast films of a 50/50 blend of PVC and NBR-26 obtained for various rates of solvent (THF) evaporation as shown in Figure 4b. The scattering peak shifts to smaller scattering angles with decreasing rate of evaporation. That is, the slower the evaporation of solvent, the larger is the periodic distance of the phase-separated morphology, as indicated in Figure 5.

Figures 6 and 7 show the changes of light scattering profiles during the slow casting process A and the quick one D, respectively. In both cases, the scattering peak appeared in the concentrated solutions. The peak angles

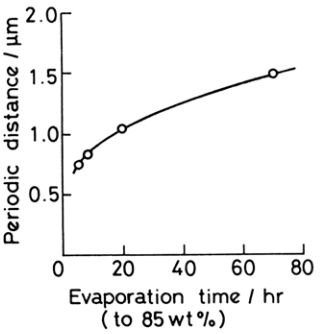

Figure 5. Dependence of periodic distance on the rate of solvent evaporation.

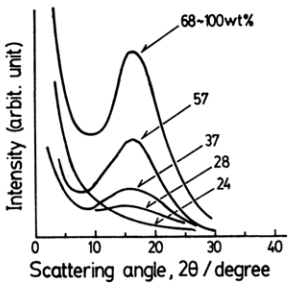

Figure 6. Change of light scattering profile during casting process A (see Figure 4b). Figures are total polymer concentrations.

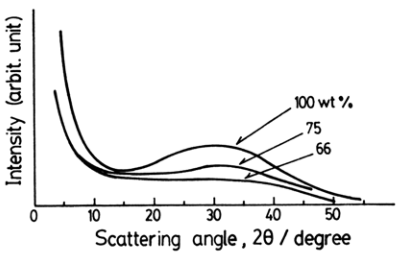

Figure 7. Change of light scattering profiles during casting process D (see Figure 4b). Figures are total polymer concentrations.

remained almost constant but scattered intensities became higher at the higher concentrations approaching neat polymer. The critical concentrations at which the scattering peaks were initially detected are shown as open circles in Figure 4b. The slower the evaporation, the lower is the critical concentration. The results imply that the regular structure formed at the critical concentration may be maintained as a whole at higher concentrations until the solid structure is formed and also that the periodic distance of the structure depends on the critical concentration.

The phenomena shown in Figure 5–7 were observed also in the other polymer–polymer pairs as will be presented later.

Hereafter we will call the phase-separated structure in Figures 2 and 3 a "modulated structure" as has been done in the fields of inorganic glasses and metals.[6,7] We use the term for convenience to describe the morphological features of unique periodicity and high level of phase connectivity.

Polymer Pairs Forming the Modulated Structure. In Figure 8 are shown some selected examples of the experimental results obtained for various pairs of polymers in Table I. Rate of solvent evaporation is indicated by t_c in Figure 8. t_c is the evaporation time needed to attain a total polymer concentration of ca. 85 wt %. In Figure 8 are shown two extreme cases: quick evaporation (small t_c) and slow evaporation (large t_c) for the respective systems.

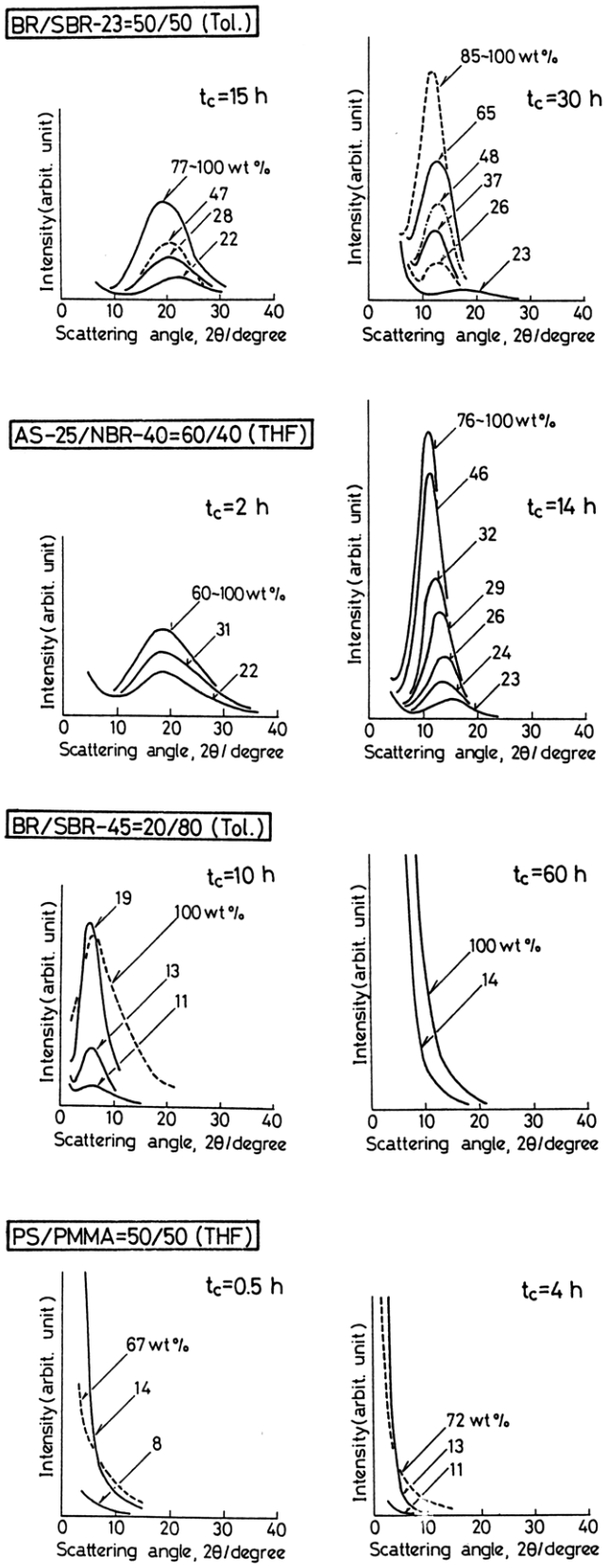

Figure 8. Changes of light scattering profiles during castings of various ternary systems. t_c is evaporation time needed to attain a total polymer concentration of ca. 85 wt %. Two extreme cases are shown for respective systems: (left) quick evaporation; (right) slow evaporation.

The BR/SBR-23/toluene and AS-25/NBR-40/THF systems show behavior similar to that of the PVC/NBR-26/THF system. In some cases, the scattering peak appearing initially at low concentrations shifts to smaller

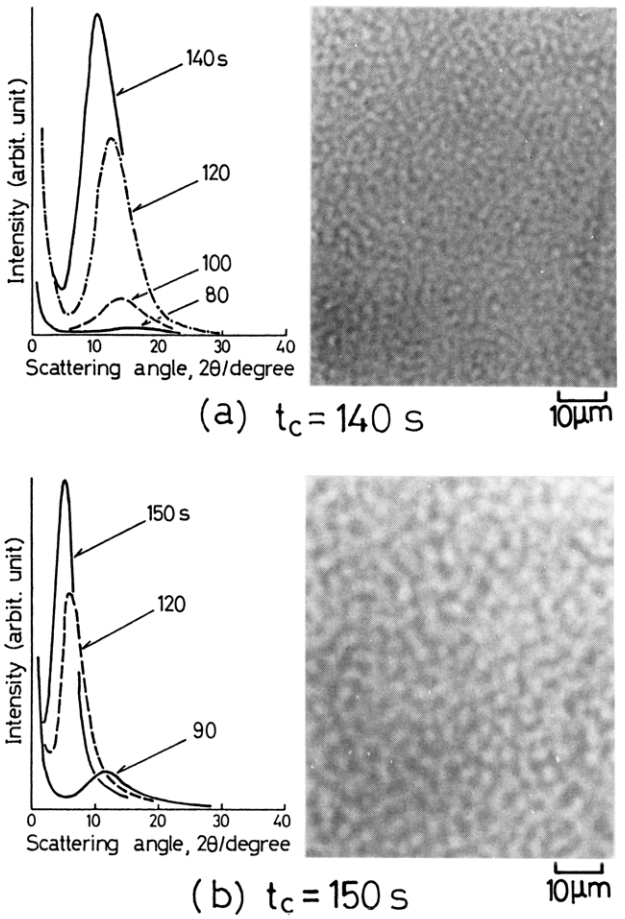

Figure 9. Changes of light scattering profiles during casting of BR/SBR-45/toluene systems and light micrographs of cast films. (a) t_c = 140 s; (b) t_c = 150 s. Figures are times after the start of solvent evaporation.

scattering angles during evaporation. This implies some degree of coarsening of the structure. The micrographs of the cast films, however, are similar to that in Figure 2, indicating the formation of a modulated structure.

Polymer pairs which have given similar results are IR/BR (toluene), CR/EVA-58 (THF), SBR-23/SBR-45 (toluene), CR/NBR-20 (THF), PVC/EVA-58 (THF), and NBR-26/NBR-32 (THF).

The BR/SBR-40/toluene system in Figure 8 formed the modulated structure with long periodic distance by the relatively quick evaporation but failed to form it by slow evaporation. The modulated structures from the much faster evaporation are demonstrated Figure 9.

The PS/PMMA/toluene system in Figure 8 failed to form the modulated structure even through the quick evaporation. Micrographs of the cast films were oridinary ones observed generally in the cast films of incompatible polymers;[8,10] isolated spherical domains of one component with diameters ranging from a few microns to ca. 50 μm are dispersed in the matrix of the other component.

Consulting the solubility parameters in Table I, we see that the polymer pairs forming the modulated structure have fairly small differences in the solubility parameters between the component polymer.

Effect of Blend Ratio. Figure 10 shows the effect of blend ratio of polymers on the development of modulated structure. The system shown in Figure 10 is BR/SBR-23/toluene. Here the rate of solvent evaporation is almost same for the respective systems (t_c = 30 h). The modulated structure was observed for every system having the blend ratio ranging from 20/80 to 80/20.

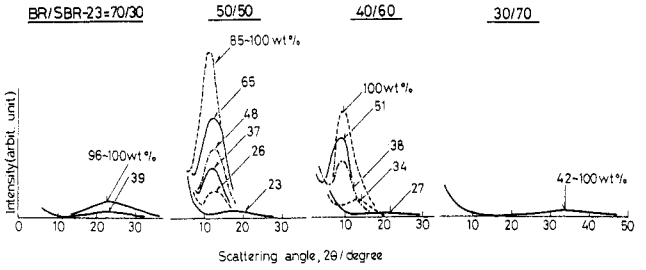

Figure 10. Changes of light scattering profiles during castings of BR/SBR-23/toluene systems having various blend ratios of polymers.

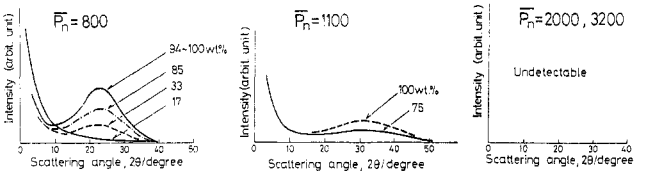

Figure 11. Changes of light scattering profiles during casting of PVC/NBR-26/THF systems having various degrees of polymerization ($\bar{P}_n$) of PVC.

In the case of symmetrical blend (50/50 blend system), the scattering peak initially appears at the lowest concentration and the final scattering peak is at the lowest scattering angle, suggesting the longest periodic distance in the modulated structure. The larger the deviation of the blend ratio from symmetry (e.g., from 50/50 to 70/30 or 30/70), the higher the concentration at which the scattering peak was initially detected and the higher the angle of final scattering peak, suggesting a shorter periodic distance in the modulated structure.

Similar results have been observed in other systems such as BR/SBR-45/toluene and AS-25/NBR-40/THF. In every system, the larger the deviation of blend ratio from symmetry, the slower is the rate of phase separation (for example, compare 70/30 and 60/40 in Figure 10).

Effect of Molecular Weight. Figure 11 shows the effect of molecular weight ($\bar{P}_n$ = degree of polymerization) of PVC on the development of the structure in the PVC/NBR-26/THF system. The evaporation rates are almost the same for the respective systems (t_c = 5 h). The smaller the $\bar{P}_n$, the lower the concentration at which the scattering peak was initially detected and the lower the angle of the scattering peak. In the systems consisting of PVC's with high $\bar{P}_n$'s (2000 and 3200), no scattering intensity was detected. These systems, however, gave a scattering peak when the evaporation was very slow, e.g., t_c = 200 h.

It seems that the $\bar{P}_n$ affects very much the diffusivity of the system and hence the rate of phase separation. That is, if the $\bar{P}_n$ is high, appreciable phase separation cannot occur during the fast casting, resulting in an almost homogeneous blend.

Discussion

We will interpret the experimental results on the development of modulated structure in terms of the thermodynamics and the kinetics of phase separation of the ternary polymer solution.

In Figure 12 is shown an example of the phase diagrams of our ternary system. The system in Figure 12 is PVC/NBR-26/THF. The solid curve in the figure is the spinodal curve calculated by the procedure of Zeman and Patterson.[12] The broken line shows the binodal curve expected for the system. The binodal separates the phase diagram into homogeneous and two-phase regions. The spinodal separates the two-phase region into the thermodynamically metastable and unstable regions.[6] In the metastable region located between the spinodal and binodal, an initially homogeneous solution separates by a nucleation and growth mechanism. In the unstable region located within the spinodal, phase separation proceeds via the spinodal decomposition mechanism.

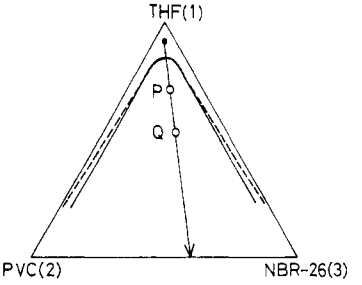

Figure 12. Phase diagram of the PVC/NBR-26/THF system. The spinodal curve is calculated by the procedure of Zeman and Patterson,[12] setting χ_{12} = 0.00282, χ_{13} = 0.00558, and χ_{23} = 0.00872. The arrow indicates the casting process.

Now think about the casting process. The initial ternary solution and the casting process are indicated by the closed circle and arrow in Figure 12, respectively. By solvent evaporation, the solution is thrust into the two-phase region in which the solution should separate into A-polymer-rich and B-polymer-rich phases. The solution has to pass through the metastable region before it is thrust into the unstable region. As has been recognized,[3,6] the nucleation and growth is a slow rate process. So, if the time to pass through the metastable region is short enough, phase separation by nucleation and growth may not happen before the solution reaches the unstable region and begins to separate by the spinodal decomposition mechanism. Our experimental results suggest that this situation must be realized in our systems forming the modulated structures. That is, both the high level of phase interconnectivity in microscopy and the light scattering peak showing the unique periodicity of the structure are the hallmarks of the spinodal decomposition, as is well-known.[6,11] The points to be discussed are the effects of molecular and processing variables on the phase separation in the unstable region.

The results shown in Figure 5, for example, may be qualitatively interpreted in terms of the relative rate of spinodal decomposition compared to that of solvent evaporation (change of total polymer concentration). That is, when the evaporation rate is fairly high, appreciable decomposition cannot occur during the casting process even in the unstable region until evaporation proceeds to the higher polymer concentration of point Q in Figure 12. At point Q, which deviates much from the spinodal curve, the rate of decomposition is high and the wavelength of the concentration fluctuation is short, as expected by the spinodal decomposition kinetics.[11] Then the fluctuation will be frozen in at the higher polymer concentrations to result in the modulated structure in the cast film. On the other hand, when the rate of evaporation is slow, the concentration fluctuation near point P (not far from the spinodal) grows sufficiently to give the morphology with a long periodic distance. These situations will be discussed more quantitatively in the following.

The familiar Flory–Huggins expression of the free energy of mixing, f, of the ternary polymer solution consisting of A polymer, B polymer, and solvent is written as[13]

$$\frac{f}{RT} = \sum_i \frac{\phi_i}{v_i} \ln \phi_i + \sum_{i<j} \chi_{ij} \phi_i \phi_j \qquad (1)$$

where i = A, B, and S (A = A polymer, B = B polymer,

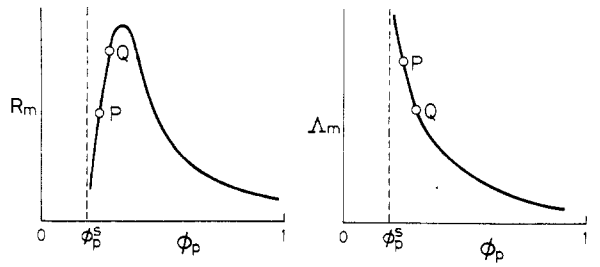

Figure 13. Concentration dependence of R_m and Λ_m. Calculated from eq 6 and 7.

and S = solvent), ϕ_i's are the volume fractions, v_i's are the molar volumes, and χ_{ij}'s are the interaction parameters. Following the procedure of Scott,[14] we define the relative volume fraction of polymers θ and the volume fraction of total polymer ϕ_P by

$$\theta_A = \phi_A/(\phi_A + \phi_B) \tag{2}$$

$$\theta_B = \phi_B/(\phi_A + \phi_B) \tag{3}$$

$$\phi_P = \phi_A + \phi_B = 1 - \phi_S \tag{4}$$

The second derivative of f with respect to θ_A is given by

$$\frac{\partial^2 f}{\partial \theta_A{}^2} = RT\phi_P\left(\frac{1}{v_A\theta_A} + \frac{1}{v_B\theta_B} - \frac{2\chi_{AB}\phi_P}{v_A}\right) \tag{5}$$

$$= -2RT\frac{\chi_{AB}}{v_A}\phi_P(\phi_P - \phi_P{}^s) \tag{5'}$$

where $\phi_P{}^s$ is the spinodal volume fraction of total polymer at which $(\partial^2 f/\partial\theta_A{}^2) = 0$. From eq 15 one can obtain the characteristic parameters describing the kinetics of phase separation such as Λ_m and R_m. Λ_m is the most probable wavelength of the fluctuation having the highest rate of growth. R_m is the maximum rate constant of fluctuation growth. The parameters are given by

$$\Lambda_m = 4\pi[-(\partial^2 f/\partial\theta_A{}^2)/4\kappa]^{-1/2} = 2\pi l[3(\phi_P - \phi_P{}^s)]^{-1/2} \tag{6}$$

$$R_m = M(\partial^2 f/\partial\theta_A{}^2)^2/8\kappa = \frac{3RT}{l^2}M\frac{\chi_{AB}}{V_A}\phi_P(\phi_P - \phi_P{}^s)^2 \tag{7}$$

where M is the mobility and κ is the gradient energy coefficient represented according to van Aartsen;[15] using the dilution approximation of Scott[14]

$$\kappa = \frac{RT\chi_{AB}\phi_P l^2}{\delta v_A} \tag{8}$$

where l is a range of polymer–polymer interaction.[15]

One of the most characteristic features of the spinodal decomposition elucidated by the linearized theory is the exponential nature of the growth rate of the composition fluctuation:

$$|\theta_A(t) - \theta_A(t = 0)| \propto \exp(R_m t) \tag{9}$$

that is, the periodic distance of the fluctuation should be dominated by R_m, and R_m can be assumed to be a rate constant of phase separation.

Figure 13 is a schematic representation of R_m and Λ_m vs. ϕ_P. In eq 7, the $\phi_P(\phi_P - \phi_P{}^s)^2$ term increases with ϕ_P and M is a decreasing function of ϕ_P; $M \sim \phi_P{}^{-4}$ is assumed in Figure 13.[16] The product of M and $\phi_P(\phi_P - \phi_P{}^s)^2$, that is, R_m, gives a curve with maximum as in Figure 13. Now let us think about again the phase separation during the casting (solvent evaporation) process, keeping in mind the exponential nature of eq 9.

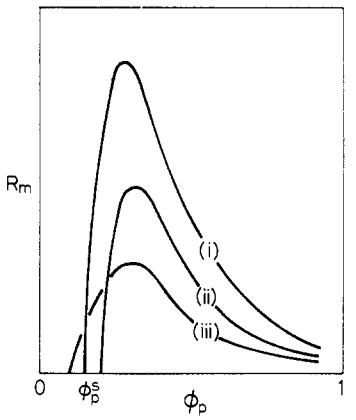

Figure 14. Concentration dependence of R_m, showing the effects of χ_{AB}, blend ratio $\theta_A\theta_B$, and degree of polymerization N: (i) larger χ_{AB}, $\theta_A \simeq \theta_B$; (ii) small χ_{AB}, $\theta_A < \theta_B$; (iii) large N.

When the rate of solvent evaporation is small, appreciable phase separation is expected to occur at low concentration, e.g., near point P in Figure 13, resulting in a large Λ_m. When the rate of evaporation is large, appreciable phase separation is not expected to occur at low concentration but is expected to occur at higher concentration, e.g., near point Q, resulting in a smaller Λ_m. That is, when the evaporation rate is fairly high, appreciable phase separation cannot occur during casting even in the unstable region, until the evaporation proceeds to the higher polymer concentration. This is a qualitative interpretation of the results that a larger rate of solvent evaporation yields a smaller periodic distance in the modulated structure, the phenomena typically shown in Figure 5.

If the evaporation is much faster, appreciable phase separation fails to occur even at the concentration with maximum R_m, resulting in a homogeneous blend, in the extreme case. This point will be discussed further in Figure 14 with respect to the effect of molecular weight on the development of structure.

Schematic curves in Figure 14 show the change of the R_m–ϕ_P relation with various factors such as the polymer–polymer interaction parameter χ_{AB}, blend ratio of polymers θ_A, and degree of polymerization N ($\bar{P}_n$). According to eq 5, the spinodal polymer volume fraction $\phi_P{}^s$ is given by

$$\phi_P{}^s \sim (\chi_{AB}\theta_A\theta_B)^{-1} \tag{10}$$

for a symmetrical polymer pair ($v_A = v_B$). So, the larger the χ_{AB}, the smaller are the $\phi_P{}^s$. Hence, as χ_{AB} increases, the R_m–ϕ_P curve shifts from (ii) to (i). This interprets the result that, for a given rate of evaporation, the polymer–polymer pair having large χ_{AB} (or $|\delta_A - \delta_B|$) fails to form the modulated structure but forms the macrophase-separated structure, as shown in Figure 8.

The situation is the same with respect to the blend ratio of polymers. The symmetrical blend of $\theta_A = \theta_B$ (50/50 blend) gives the maximum of the product $\theta_A\theta_B$. The larger the deviation from the symmetry, the smaller is the product $\theta_A\theta_B$, and hence the larger is the $\phi_P{}^s$. Thus, the deviation of blend ratio from symmetry shifts the R_m–ϕ_P curve from (i) to (ii). This interprets the results shown in Figure 10.

According to eq 7, the degree of polymerization N affects $R(q_m)$ in terms of l, $\phi_P{}^s$, and M. $\phi_P{}^s$ decreases with increasing N; $\phi_P{}^s \sim N^{-1}$ for the symmetrical pair ($v_A = v_B$), for example. l^2 is approximately twice the radius of gyration ($2R_g{}^2$).[15] Hence l^2 is proportional to N^2. The power law of $M \sim N^{-2}$ may be appropriate for our ternary system, as has been predicted theoretically[19] and has been verified

by forced Rayleigh scattering and dynamic light scattering studies.[20,21] The effects of l^2 and M on R_m ($\sim N^{-4}$) prevail over that of ϕ_P^s ($\sim N^{-1}$), resulting in curve (iii) with low magnitude of R_m. Thus the homogeneous blend without appreciable composition fluctuation is expected in the ternary system consisting of very high molecular weight polymers, unless sufficient time to phase-separate is given. We think the situation is realized in Figure 11.

Concluding Remarks

We have found the development of modulated structure in solution-cast films of polymer blends. Characteristic features of the structure are the high level of phase interconnectivity and the unique periodicity. We have investigated the effects of various factors on the development of modulated structure: casting speed, polymer–polymer compatibility, blend ratio of polymers, and molecular weights of polymers. The experimental results have been interpreted in terms of the thermodynamics of ternary polymer solution and the kinetics of spinodal decomposition.

Our arguments have come from the assumption that the prevailing mechanism of phase separation during the solution casting is the spinodal decomposition. The assumption has been based on the morphological features. To verify the assumption in a quantitative sense, we should rely upon the kinetic studies of phase separation in ternary systems. The kinetic studies are under way using a temperature-drop procedure instead of the concentration jump corresponding to the solution casting. The results will be published elsewhere.[22]

Formation of the modulated structure in polymer blends has been limited to the thermally induced phase separation of the two-component polymer systems having LCST and UCST type phase diagrams.[3-5] We believe that our studies have presented a new way to prepare polymer blends with modulated structure for various polymer pairs. On the other hand, this type of study is very important in the estimation procedures of polymer–polymer compatibility, which is commonly based upon the morphological investigations and measurements of physical properties of solution-cast films of polymer blends. That is, attention should be paid to the time scale of film preparation for the proper estimation of polymer–polymer compatibility.

Acknowledgment. We acknowledge partial support by the Scientific Research Fund (Kagaku-Kenkyu-hi 58470079) of the Ministry of Education, Japan, and grants from Shinsei-shigen-kyokai, Tokyo, Japan, and the Japan Synthetic Rubber Co. Ltd., Tokyo, Japan.

Registry No. Poly(vinyl chloride) (homopolymer), 9002-86-2; poly(acrylonitrile-*co*-styrene), 9003-54-7; poly(ethylene-*co*-vinyl acetate), 24937-78-8; poly(methyl methacrylate) (homopolymer), 9011-14-7; polystyrene (homopolymer), 9003-53-6.

References and Notes

(1) Yasuda, O.; Ougizawa, T.; Inoue, T.; Miyasaka, K. *J. Polym. Sci., Polym. Lett. Ed.* **1983**, *21*, 813.
(2) Inoue, T.; Kobayashi, T.; Hashimoto, T.; Tanigami, T.; Miyasaka, K. *Polymer*, in press.
(3) McMaster, L. P. *Adv. Chem. Ser.* **1975**, *No. 142*, 43.
(4) Nishi, T.; Wang, T. T.; Kwei, T. K. *Macromolecules* **1975**, *8*, 227.
(5) Nojima, S.; Tsutsumi, K.; Nose, T. *Polym. J.* **1982**, *14*, 225.
(6) Cahn, J. W. *Trans. Metall. Soc. AIME* **1968**, *242*, 166.
(7) Hilliard, H.; Cohen, M.; Averbach, B. L. *Acta Metall.* **1961**, *9*, 536.
(8) Gardiner, J. B. *Rubber Chem. Technol.* **1970**, *43*, 370.
(9) Stein, R. S.; Rhodes, M. B. *J. Appl. Phys.* **1960**, *31*, 1873.
(10) A recent example is given by: Eastmond, G. C.; Jiang, M.; Malinconico, M. *Polymer* **1983**, *24*, 1162.
(11) Cahn, J. W. *J. Chem. Phys.* **1965**, *42*, 93.
(12) Zeman, K.; Patterson, D. *Macromolecules* **1972**, *5*, 513.
(13) Flory, P. "Principles of Polymer Chemistry"; Cornell University Press: Ithaca, NY, 1953.
(14) Scott, R. L. *J. Chem. Phys.* **1949**, *17*, 274.
(15) van Aartsen, J. J. *Eur. Polym. J.* **1970**, *6*, 919.
(16) Lodge[17] and Wesson et al.[18] have shown that the concentration dependence of the self-diffusion coefficient D_s of a polymer chain in solution is not described by a unique power law such as $D_s \sim c^{-1.75}$ (in good solvent) nor $D_s \sim c^{-3.0}$ (in Θ solvent) as described by scaling arguments (developed by de Gennes) but the slopes of log D_s–log c plots are steeper than expected, especially in concentrated solutions. Here we assumed a −4 power law only to simplify the discussion.
(17) Lodge, T. P. *Macromolecules* **1983**, *16*, 1393.
(18) Wesson, J. A.; Noh, I.; Kitano, T.; Yu, H. *Macromolecules* **1984**, *17*, 782.
(19) de Gennes, P.-G. *Macromolecules* **1976**, *9*, 594.
(20) Leger, L.; Hervet, H.; Rondelez, F. *Macromolecules* **1981**, *14*, 1732.
(21) Amis, E. J.; Han, C. C. *Polymer* **1982**, *23*, 1403.
(22) A part of the kinetic studies has been presented at the 32nd Polymer Symposium, Society of Polymer Science, Japan, Oct 1983, showing that the kinetics of phase separation can be described by the spinodal decomposition theory.

Structural Studies of Poly(*N*-vinylimidazole) Complexes by Infrared and Raman Spectroscopy

Joseph L. Lippert,* John A. Robertson, John R. Havens, and Julia S. Tan*

Eastman Kodak Company, Research Laboratories, Rochester, New York 14650.
Received December 29, 1983

ABSTRACT: Structural changes of poly(*N*-vinylimidazole) induced by metal complexation and protonation have been studied by Fourier-transform infrared and Raman spectroscopy. Ni^{2+} complexation was indicated by shifts of the imidazole ring-mode vibrational bands at 1500, 1085, and 915 cm^{-1} to higher frequencies. Spectral changes in the N–H stretching region (2400–2900 cm^{-1}) and the ring-mode deformation at 915 cm^{-1} are consistent with the formation of an H-bridged complex between the protonated and unprotonated imidazole rings upon partial protonation. These latter changes are accompanied by an intensity change in the Raman band at 1015–1020 cm^{-1}, which is suggested to be associated with a conformational change in the chain backbone.

The solution behavior of poly(*N*-vinylimidazole) has been well characterized and reported from these laboratories.[1,2] These studies show that the conformation of the polymer chain is sensitive to the degree of protonation, the degree of quaternization, the nature of the solvent, and the type of added salts. It is believed that both overall and

0024-9297/85/2218-0063$01.50/0